FULL PAPERS

Magnetic Resonance in Medicine 46:451–456 (2001)

In Vivo ^{1}H NMR Spectroscopy of the Human Brain at 7 T

Ivan Tkáč,* Peter Andersen, Gregor Adriany, Hellmut Merkle, Kâmil Uğurbil, and Rolf Gruetter

In vivo ^{1}H NMR spectra from the human brain were measured at 7 T. Ultrashort echo-time STEAM was used to minimize J-modulation and signal attenuation caused by the shorter T_2 of metabolites. Precise adjustment of higher-order shims, which was achieved with FASTMAP, was crucial to benefit from this high magnetic field. Sensitivity improvements were evident from single-shot spectra and from the direct detection of glucose at 5.23 ppm in 8-ml volumes. The linewidth of the creatine methyl resonance was at best 9 Hz. In spite of the increased linewidth of singlet resonances at 7 T, the ability to resolve overlapping multiplets of J-coupled spin systems, such as glutamine and glutamate, was substantially increased. Characteristic spectral patterns of metabolites, e.g., *myo*-inositol and taurine, were discernible in the in vivo spectra, which facilitated an unambiguous signal assignment. Magn Reson Med 46: 451–456, 2001. © 2001 Wiley-Liss, Inc.

Key words: ^{1}H NMR spectroscopy; high magnetic field; resolution; human brain

NMR spectrometers, operating at ultrahigh magnetic fields of 14–21 T, are routinely used for structural studies of complex molecules such as proteins or nucleic acids (1). However, the development of in vivo high-field NMR spectroscopy was delayed due to hardware limitations, such as the availability of wide-bore magnets, increased demands on gradient performance, and a lack of efficient methods to correct the B_0 field inhomogeneity induced by the subject (shimming). Today, most of the clinical MR scanners equipped with spectroscopy packages operate at 1.5 T. In addition to N-acetylaspartate (NAA), creatine (Cr), choline (Cho), and lactate (Lac), quantification of other metabolites such as *myo*-inositol (Ins) and glutamate/glutamine was reported in short echo-time spectra (2,3). Increased accuracy and reliability of quantification was achieved at 2 T (4), which allowed the assessment of regional changes of brain metabolites, including N-acetylaspartylglutamate (NAAG) (5).

Preliminary results obtained in the late 1980s demonstrated the feasibility of in vivo ^{1}H NMR spectroscopy of human brain at 4 T and confirmed the expected increased sensitivity (6,7). Nonlinear field deformations induced by susceptibility differences between air and tissue at 4 T were not correctable by linear shims alone. Gruetter et al. have shown that adjustment of all first- and second-order shims by FASTMAP (fast, automatic shimming technique by mapping along projections) (8) resulted in significantly improved spectral resolution at 4 T relative to 1.5 T, yielding partially resolved glutamine and glutamate signals (9). Increased spectral dispersion at 4 T enabled the direct detection of a glucose signal at 5.23 ppm for the first time, even at very low concentration (10). Recent comparisons of short echo-time ^{1}H NMR spectroscopy at 1.5 T and 4 T confirmed that a nearly fourfold increase in quantification precision can be achieved at the higher field for J-coupled metabolites such as glutamate (Glu), glutamine (Gln), and γ-aminobutyric acid (GABA) (11). T_1 relaxation times of metabolites (NAA, Cr, Cho) at 4 T (12) were found to be only slightly larger than those reported at 1.5 T. However, apparent T_2-values were significantly shorter (12,13) than at 1.5 T. Increased sensitivity at 4 T has allowed increased spatial resolution in spectroscopic imaging (SI), which resulted in the evaluation of metabolite concentration differences between gray and white matter based on image segmentation (14,15). Increased signal separation at 4 T minimized the contamination of glutamate and GABA signals by unwanted resonances when measured by homonuclear editing techniques (16,17).

Magnetic fields higher than 4 T have been employed in ^{1}H spectroscopy studies of animal brains. In vivo ^{1}H NMR spectroscopy at 7 T was used to quantify metabolite concentrations in the brain of gerbils (18) and to monitor the changes during and after acute hypoxia-ischemia in newborn piglets (19). Spatial distribution of a limited number of metabolites was assessed in rat brain using 2D and 3D SI (20,21). The 2D-spatial/2D-spectral SI technique was used to improve the resolution of spectra measured from intracerebral gliomas in rat brain (22). However, limited spectral resolution resulting from uncompensated B_0 gradients was a common feature of all aforementioned experiments performed on animals at 7 T. Gruetter et al. (9) demonstrated that spectra with excellent resolution can be measured also in vivo at 9.4 T, when all first- and second-order shim terms were correctly set by FASTMAP (8,9). Subsequently, Pfeuffer et al. (23) showed that quantification of 18 metabolites in rat brain at 9.4 T was possible when FASTMAP shimming (8,9), highly efficient water suppression (24), ultrashort echo-time STEAM (TE = 1 ms) (24), and LCModel data processing (25) were combined. In addition to commonly measured metabolites such as total creatine, NAA, Cho, Glu, Gln, Lac, and Ins, concentrations of alanine (Ala), aspartate (Asp), glutathione (GSH), GABA, phosphorylethanolamine (PE), and taurine (Tau) were quantified. The resolved signals of methylene groups

Center for Magnetic Resonance Research, University of Minnesota, Minneapolis, Minnesota.

Grant sponsor: National Institutes of Health; Grant number: P41RR08079; Grant sponsors: W.M. Keck Foundation; National Foundation for Functional Brain Imaging.

*Correspondence to: Ivan Tkáč, Ph.D., Center for Magnetic Resonance Research, Department of Radiology, University of Minnesota, 2021 6th Street SE, Minneapolis, MN 55455. E-mail: ivan@cmrr.umn.edu

Received 31 January 2001; revised 14 March 2001; accepted 2 April 2001.

of Cr and PCr were clearly discernible in ^{1}H NMR spectra of rat brain.

The purpose of this article is to report preliminary results concerning the sensitivity and resolution of ^{1}H MRS in the human brain using a whole-body 7 T magnet.

METHODS

A total of 18 subjects were studied after giving informed consent according to procedures approved by the Institutional Review Board and the FDA. The measurements were performed on a 7 T / 90 cm magnet (Magnex Scientific, Abingdon, UK) with a head gradient coil (40 mT/m, 500 μs) and a Turbo/Ultra gradient power amplifier (Siemens AG, Medical Engineering, Erlangen, Germany) interfaced to a Varian INOVA console (Varian, Palo Alto, CA). A shielded quadrature transmit/receive surface RF coil (26) consisting of two geometrically decoupled single-turn coils with 12-cm diameter each was used to measure spectra from the occipital lobe. To measure spectra from the parietal white matter, a circularly polarized helmet RF coil (27) was used. All first- and second-order shim terms were adjusted based on a recently improved FASTMAP sequence using EPI readout (28). The water signal was suppressed by eight variable power RF pulses with optimized relaxation delays (VAPOR) (24). Transmitter power of the fifth water suppression RF pulse was increased by 4 dB, the powers of the third, seventh, and eighth pulse were increased by 5 dB relative to the nominal RF power used for water suppression. The following interpulse delays were used in VAPOR: 150 ms – 100 ms – 122 ms – 105 ms – 102 ms – 61 ms – 67 ms – 14 ms. Three outer volume suppression (OVS) blocks, each consisting of six hyperbolic-secant RF pulses (8 kHz bandwidth) were interleaved with water suppression pulses. An ultrashort echo-time STEAM localization sequence with asymmetric RF pulses (24) was adapted to the 7-T system. The displacement error was reduced by using the highest RF power (2.3 kW) currently available at the RF coil port. The resulting peak amplitude of RF field (B_1) in the selected volume of interest (VOI) of the brain ($\gamma B_1/2\pi$ = 1.1–1.5 kHz, where γ is the gyromagnetic ratio) limited the shortest achievable duration of the asymmetric RF pulses to 1.5 ms (4.5 kHz bandwidth) and shortest echo time to 6 ms. The position of the VOI in the occipital lobe was chosen based on FLASH images. Power absorption (SAR) was well within FDA guidelines.

RESULTS

Automatically adjusted shim currents never reached maximum settings due to the strong shim coils specifically designed for this 7 T magnet. Shimming resulted in water linewidths of 11–13 Hz with a concomitant creatine linewidth of 9–11 Hz. To minimize the effect of drifting B_0 or subject movement on signal line width, data were always acquired as a series of FIDs (consisting of 16 averages each) that were saved in memory separately. The FIDs were individually corrected for frequency drift and then summed together and processed (weighted FT and zero-order phase correction). Further improvements were not noticeable when data were acquired as an array of single-shot FIDs and when each FID was corrected for frequency drift before summation. Approximately a twofold increase in RF power was necessary at 7 T relative to 4 T to achieve the same peak B_1 in the same location of the brain, using RF coils of the same design and similar loop size. The short echo-time (TE = 6 ms) minimized signal attenuation due to T_2 relaxation and J-modulation effects. The single-shot ^{1}H NMR spectrum measured from an 8-ml volume located in occipital lobe (Fig. 1, top trace) demonstrated increased sensitivity at 7 T. Approximately a twofold increase in SNR was observed at 7 T relative to spectra acquired at 4 T. In an averaged spectrum, the H-1 α-glucose signal at 5.23 ppm was detectable (Fig. 1, bottom trace) in healthy subjects without exogenous glucose administration. In spite of an ultrashort TE of 6 ms, very broad signals and baseline distortions were not observed.

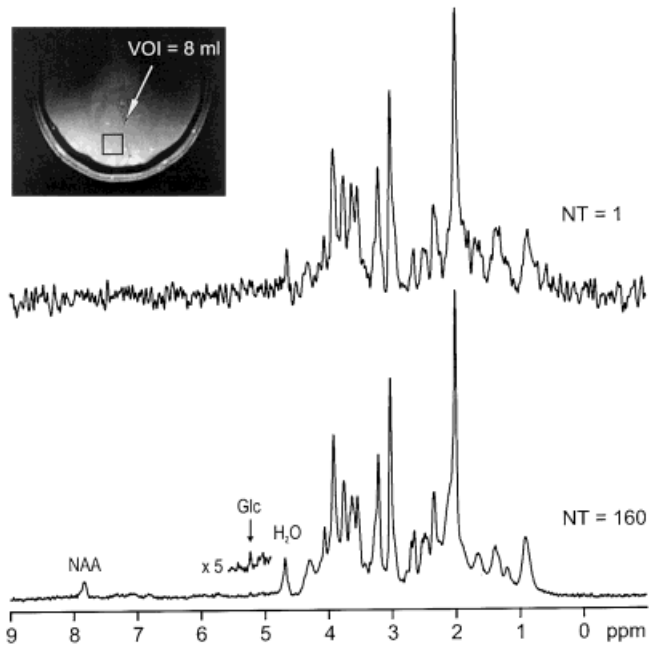

FIG. 1. In vivo ^{1}H NMR spectra of human brain (occipital gray matter) measured at 7 T by the STEAM sequence with VAPOR water suppression (24) using a quadrature transmit/receive surface RF coil (26). Single shot spectrum, number of transients NT = 1 (top trace), averaged spectrum, NT = 160 (bottom trace). TE = 6 ms, TM = 32 ms, TR = 5 s, VOI = 8 ml. After Gaussian multiplication (gf = 0.1) of FID and FT only zero-order phase correction applied. Inset: gradient echo MRI with the location of VOI, transverse slice.

The expanded region of a ^{1}H NMR spectrum measured from occipital gray matter (Fig. 2) demonstrates improvements in spectral resolution achievable at 7 T. The glutamate and glutamine resonances at 2.35 and 2.45 ppm were clearly separated. In addition to the strong signals from NAA, Ins, Glu, and total Cr, signal contributions from aspartate (2.8 ppm), GABA (2.28 ppm), PE (3.98 ppm), and *scyllo*-inositol (scyllo-Ins, 3.34 ppm) (29) were discernible in the 7 T spectra. The upfield shoulder at the position of the Cr methyl signal can be assigned to glutathione and underlying macromolecule resonances. An expanded part of the in vivo spectrum was compared to the spectra of Tau, glucose, and Ins measured in phantoms (Fig. 2, top). All resonances of Ins in the in vivo spectrum were in

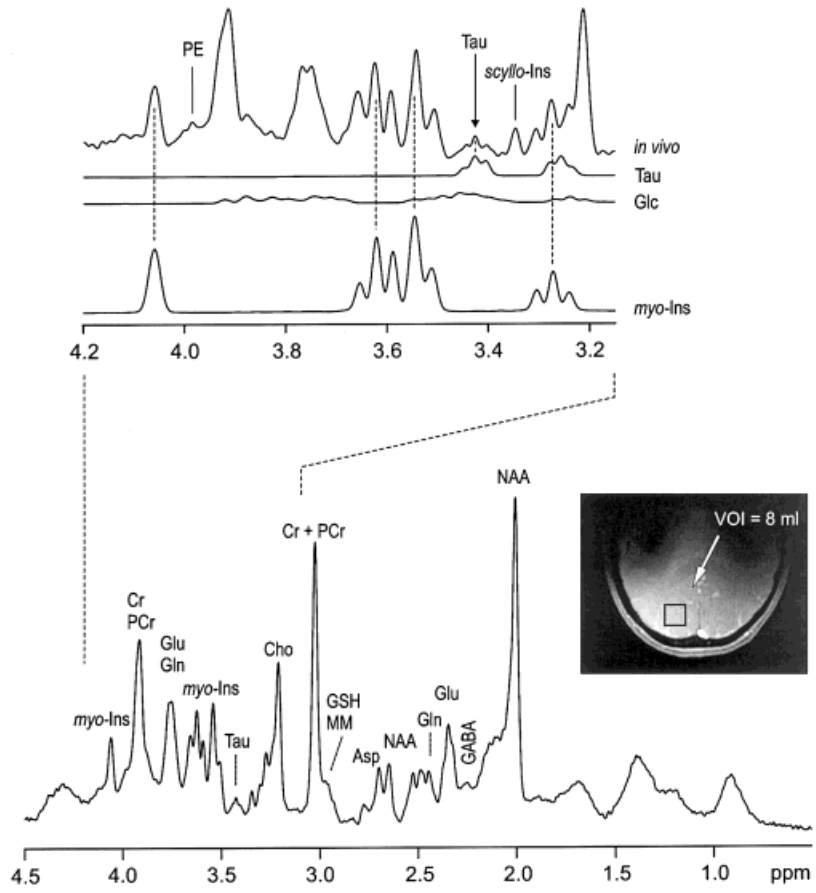

FIG. 2. In vivo ^{1}H NMR spectrum from occipital lobe measured at 7 T. STEAM, TE = 6 ms, TM = 32 ms, TR = 5 s, VOI = 8 ml, NT = 160, resolution enhancement by shifted Gaussian function gf = 0.15 and gfs = 0.08 (bottom trace). Top: expanded part of the in vivo spectrum (gf = 0.10 and gfs = 0.10) compared to line-broadened solution spectra of taurine, glucose, and *myo*-inositol. Inset: transverse gradient echo MRI with the location of VOI, obtained with a quadrature transmit/receive surface RF coil (26).

excellent agreement with the solution spectrum. The glucose spectrum was scaled according to the H-1 signal of α-Glc at 5.23 ppm (not shown). The peak at 3.42 ppm in the spectrum from the brain corresponded to the chemical shift of the SCH_2 group of Tau and was clearly different from the glucose signal at 3.45 ppm. The concentration of Tau in occipital gray matter was estimated to be ~1.5 μmol/g. In addition, the line-shape of the creatine/phosphocreatine signal at 3.92 ppm was non-Lorentzian and asymmetric and the linewidth was clearly different from that of the methyl resonance at 3.03 ppm. A resolved signal NAAG, observed in a parietal white matter spectrum (Fig. 3), was another demonstration of improved signal separation at 7 T. The signal of resting Lac at 1.32 ppm was detectable in some spectra (Fig. 3).

In order to estimate the best linewidth achievable at 7 T in adult human brain spectra, the Hahn transverse relaxation times, T_2, of methyl protons of Cr and NAA were measured along with the best achievable linewidth of the creatine methyl resonance. A series of ^{1}H NMR spectra obtained at echo times ranging from 10–250 ms were measured from occipital gray matter of three subjects in order to assess the T_2 relaxation times of the methyl groups of NAA and Cr (Fig. 4). Signals of NAA and Cr were quantified using spectrometer built-in peak fitting procedures, while the frequencies and linewidths of the underlying broad resonances were kept fixed. The signal integrals as a function of TE were fitted with a single exponential function. The T_2 of the methyl protons of NAA was 141 ± 11 ms (mean ± SE, n = 3) and 87 ± 5 ms for the methyl protons of Cr plus PCr. The linewidth $\Delta\upsilon_{1/2}$ can be decomposed into a contribution from T_2 and microscopic and macroscopic susceptibility ($\Delta\upsilon^*$ and $\Delta\upsilon_{macro}$, respectively) according to:

$$\Delta\nu_{1/2} = \frac{1}{\pi \cdot T_2} + \Delta\nu^* + \Delta\nu_{\text{macro}}.$$

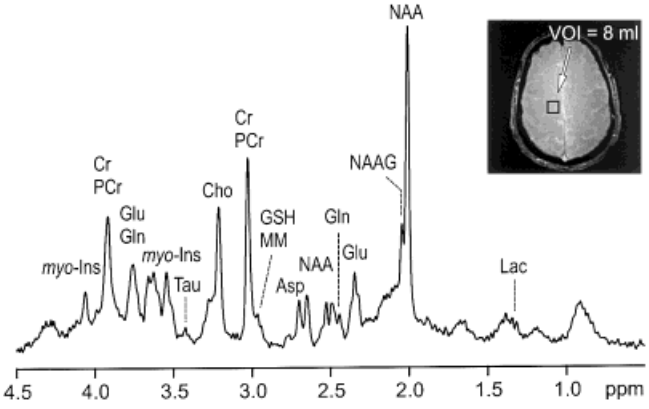

FIG. 3. In vivo ^{1}H NMR spectrum from parietal white matter measured at 7 T. STEAM, TE = 6 ms, TM = 32 ms, TR = 5 s, VOI = 8 ml, NT = 160, resolution enhancement by shifted Gaussian function (gf = 0.15 and gfs = 0.08). Inset: gradient echo transverse MRI with the location of VOI, obtained with a circularly polarized helmet RF coil (27).

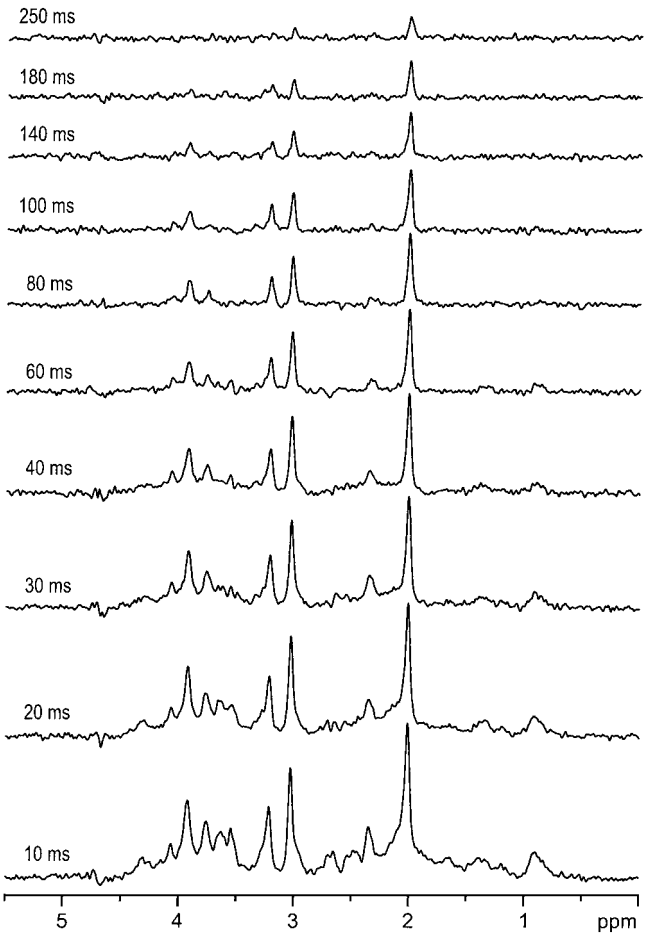

FIG. 4. In vivo ^{1}H NMR spectra from occipital lobe measured at different echo times TE = 10–250 ms. STEAM, TM = 32 ms, TR = 5 s, VOI = 8 ml, NT = 8. Processing: Gaussian multiplication (gf = 0.10), FT, and zero-order phase correction.

Table 1
Linewidths of Methyl Resonance of Total Creatine at 4 T and 7 T and Their Decompositions Into Contributions From T_2 and Microscopic Susceptibility Variations

B_0 (T)	$\Delta\nu_{1/2}$ (Hz)	$1/(\pi T_2)$ (Hz)	$\Delta\nu^*$ (Hz)
4	5.5	2.3	3.2
7	9.5	3.7	5.8

$\Delta\nu_{1/2}$ = experimentally measured linewidth of Cr at 4 T and 7 T.
$1/(\pi T_2)$ = contribution of the Hahn T_2 to the linewidth of total creatine signal at 3.03 ppm, T_2 at 7 T was experimentally measured in this study, T_2 at 4 T was set to 140 ms according to previous reports (10,12,13).
$\Delta\nu^*$ = line-broadening due to microscopic susceptibility variation calculated as $(\Delta\nu_{1/2} - 1/\pi T_2)$.

Based on the observation that the water $\Delta\upsilon_{1/2}$ was independent of voxel size (from 1–8 ml), we assumed that the macroscopic susceptibility term ($\Delta\upsilon_{macro}$) was eliminated by FASTMAP shimming. The microscopic susceptibility term, $\Delta\upsilon^*$, which leads to magnetization dephasing and additional line broadening, was calculated from the experimentally determined $\Delta\upsilon_{1/2}$ and T_2. The linewidths of Cr at 4 and 7 T and the contributions from T_2 and $\Delta\upsilon^*$ are summarized in Table 1. In conjunction with the $\Delta\upsilon_{1/2}$ and the T_2 measurements at both fields, it was possible to estimate whether the observed linewidth at 7 T was consistent with the 7/4 increase expected for $\Delta\upsilon^*$ and the experimentally measured modest decrease of T_2 at 7 T. The observed $\Delta\upsilon^*$ at 7 T was 1.8 times higher than at 4 T, which was within 5% of the expected increase.

To demonstrate the improvement in resolution for different J-coupled spin-systems, spectra of glutamate and glutamine at 1.5, 4, and 7 T were simulated (Fig. 5) using published values of chemical shifts and J-couplings (30) and standard Varian simulation software. The overall widths of the multiplets are predominantly determined by the coupling patterns and the magnitudes of homonuclear spin–spin coupling constants, as long as the $\Delta\upsilon_{1/2}$ of singlet resonances are comparable to the J-couplings constants. Therefore, in spite of the increased linewidths of singlet resonances at 7 T, the spectral resolution for coupled spin systems such as Gln and Glu was substantially improved.

DISCUSSION

A short echo-time localization sequence, originally developed for localized proton NMR spectroscopy of animals at 9.4 T with a TE of 1 ms, was adapted to a whole-body 7-T system. Despite the reduced RF field and gradient strength relative to the animal system, an echo time of 6 ms was achieved, which minimized T_2 losses and J-coupling effects. The highest accessible peak B_1 was the limiting factor for the reduction of the chemical displacement error. The highest achievable bandwidth for the asymmetric slice-selective RF pulses resulted in a 20% displacement

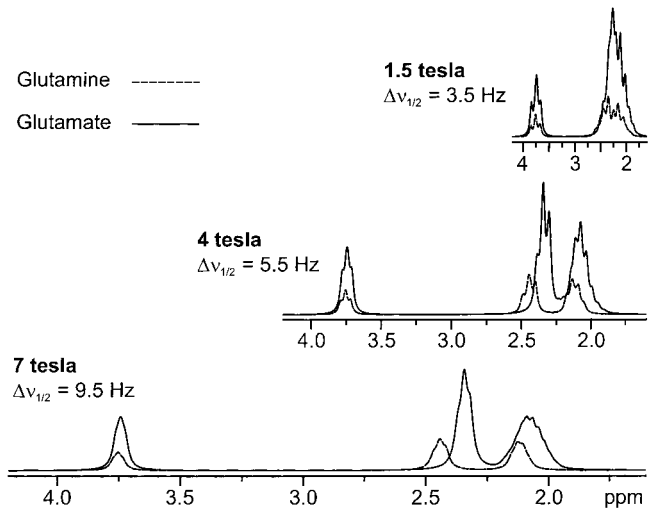

FIG. 5. Simulated ^{1}H NMR spectra of glutamine and glutamate at different magnetic field strengths. Linewidths ($\Delta\upsilon_{1/2}$) corresponded to values typical for very well shimmed volumes of the human brain. The concentration ratio [Glu]/[Gln] was set to 3 (5,11). Chemical shifts and J-coupling constants were taken from Ref. (30). Frequency scale (Hz) is identical in all three spectra.

of the voxel along each dimension for signals separated by 3 ppm.

The short echo-time of 6 ms was possible due to asymmetric RF pulses, which were used for voxel selection as in our previous study (24). The short echo-time required fine adjustment of the preemphasis to minimize eddy current effects on signal line-shapes. This was achieved using quantitative mapping methods (31). Localization performance of the sequence was improved by outer volume suppression, which reduced potential imperfections of slice selection pulses in STEAM and eliminated the contamination of spectra with signals originating outside of the VOI. Broadband (8 kHz) hyperbolic secant RF pulses used in OVS guaranteed that the displacement of slabs saturated by OVS was similar to the displacement of the VOI selected by STEAM, i.e., off-resonance signals in the VOI were not partially suppressed by OVS. Short echo-time STEAM combined with OVS and highly efficient VAPOR water suppression (24) resulted in a flat baseline (Fig. 1) achieved *without* any further postacquisition correction, such as water signal removal and baseline correction. The high frequency-selectivity of the water suppression was demonstrated by the reliable detection of the α-glucose signal (5.23 ppm) in close proximity to the water resonance.

To take advantage of the increased chemical shift dispersion at 7 T, shimming was crucial. FASTMAP shimming resulted in convergence of all first- and second-order shim terms in 3–4 iterations. The linewidth independence of the volume size (from 8 ml to 1 ml) implied that the shimming was optimal. The best linewidths observed for water signals were 12 Hz and 11 Hz in voxels located in gray and white matter, respectively. Corresponding Cr linewidths were approximately 2 Hz narrower. The calculated microscopic susceptibility terms, $\Delta\upsilon^*$, for the Cr signals at 4 and 7 T (Table 1) were in agreement with the predicted proportionality to B_0. From this comparison we estimate that a linewidth of ~9 Hz may be the resolution limit for ^{1}H NMR spectroscopy of adult human brain at 7 T. In anesthetized rat brain at 9.4 T, similar linewidths were observed, even though larger values were expected. The T_2 values of metabolites appear to be in general longer in rat brain than in human brain, e.g., Cr T_2 of 180 ms in rat brain at 4.7 T (32) vs. 140 ms in human brain at 4 T (10,12,13). However, those differences in T_2 cannot fully explain the observed differences in the linewidth. The anesthetized rat and the nonanesthetized human brain are expected to be different with respect to microscopic susceptibility variations between tissue and deoxyhemoglobin-containing blood vessels. For example, in the anesthetized rat, oxygen extraction is reduced and hence oxygenation of blood is increased (33). Differences with respect to vascular architecture between the rat and human brain may also contribute to different microscopic field inhomogeneity effects.

The single-shot spectrum obtained from an 8-ml volume of the human brain (Fig. 1) illustrates improved sensitivity at 7 T. Additional demonstration of increased sensitivity at 7 T was the direct detection of the glucose signal at 5.23 ppm from an 8-ml brain volume of normal subjects without using glucose infusion. At 4 T, significantly larger volumes were required using the same number of averages (34).

In spite of a modestly increased linewidth at 7 T, improvements in spectral resolution were evident, due to the increased separation between signals of coupled spins. For several metabolites, such as Ins and Tau, characteristic spectral patterns were discernible in the in vivo spectrum (Fig. 2), which facilitated an unambiguous signal assignment. Resolved multiplet patterns can be considered "fingerprints" of metabolites, permitting accurate assignments as well as reliable quantification. The quantification of in vivo ^{1}H NMR spectra is thus expected to be more robust and accurate, if it is based on a unique spectral pattern of multiple peaks and if the resonances do not collapse into a singlet. Improved resolution at 7 T was therefore most significant for metabolites with J-coupled spin systems, such as glutamine and glutamate (Fig. 5). The resolution improved because the overall signal widths of the overlapping multiplets were mainly determined by the homonuclear J-coupling constants, which are independent of B_0. Increased separation of signals corresponding to the H-4 protons of Glu (2.35 ppm) and Gln (2.45 ppm) is a prerequisite for a reliable quantification of those metabolites in the brain, as illustrated by the simulations in Fig. 5. Precise in vivo quantification of Glu and Gln in the brain is important, in view of recent studies based on measurements of Glu/Gln cycling between neurons and glia (35,36) and on the diagnostic and prognostic value of cerebral Gln signals in metabolic and neurodegenerative disorders (37).

The improved spectral resolution at 7 T is demonstrated in Fig. 2 (top trace). In addition to strong resonances of *myo*-Ins, Glu, Gln, Cho, and total Cr, signals of *scyllo*-Ins and Tau are clearly discernible due to good S/N ratio. Taurine concentration was estimated at 1.5 μmol/g, which is in good agreement with published data (38). As a result of highly efficient water suppression, FASTMAP shimming and excellent localization performance, detection of metabolite signals close to the water resonance, such as phosphorylethanolamine, was possible (Fig. 2), similar to rat brain spectra measured at 9.4 T (23). The methylene resonances of creatine and phosphocreatine have slightly different chemical shifts, 3.91 ppm and 3.93 ppm, respectively. In the spectra measured at 7 T, the signal at 3.92 ppm was clearly broader than the methyl resonance of Cr at 3.03 ppm, indicating the potential to quantify both metabolites separately, as described in rat brain at 9.4 T (23). The methyl resonance of NAAG was clearly resolved in a spectrum from parietal white matter (Fig. 3). In a well-shimmed spectrum measured at 2 T, the NAAG resonance was observed only as a downfield shoulder of a strong NAA peak (5). Increased separation of signals at 7 T should allow more reliable discrimination between NAA and aspartate resonances in a region between 2.4–2.9 ppm and should permit the direct detection of low concentration metabolites such as GABA or GSH without editing.

In summary, we conclude that in vivo ^{1}H NMR spectroscopy of the human brain at 7 T leads to increased sensitivity and spectral resolution, which allows unambiguous signal assignment and quantification with increased reliability.

REFERENCES

1. Wider G, Wüthrich K. NMR spectroscopy of large molecules and multimolecular assemblies in solution. Curr Opin Struct Biol 1999;9:594–601.
2. Frahm J, Bruhn H, Gyngell ML, Merboldt KD, Hänicke W, Sauter R. Localized proton NMR spectroscopy in different regions of the human brain in vivo. Relaxation times and concentrations of cerebral metabolites. Magn Reson Med 1989;11:47–63.
3. Kreis R, Ernst T, Ross BD. Absolute quantitation of water and metabolites in the human brain. II. Metabolite concentrations. J Magn Reson, Ser B 1993;102:9–19.
4. Michaelis T, Merboldt KD, Bruhn H, Hänike W, Frahm J. Absolute concentrations of metabolites in the adult human brain in vivo: quantification of localized proton MR spectra. Radiology 1993;187:219–227.
5. Pouwels PJW, Frahm J. Regional metabolite concentrations in human brain as determined by quantitative localized proton MRS. Magn Reson Med 1998;39:53–60.
6. Barfuss H, Fischer H, Hentschel D, Ladebeck R, Oppelt A, Wittig R, Duerr W, Oppelt R. In vivo magnetic resonance imaging and spectroscopy of humans with a 4 T whole-body magnet. NMR Biomed 1990;3:31–45.
7. Langkowski JH, Wieland J, Bomsdorf H, Leibfritz D, Westphal M, Offermann W, Maas R. Pre-operative localized in vivo proton spectroscopy in cerebral tumors at 4.0 Tesla—first results. Magn Reson Imaging 1989;7:547–555.
8. Gruetter R. Automatic, localized in vivo adjustment of all first- and second-order shim coils. Magn Reson Med 1993;29:804–811.
9. Gruetter R, Weisdorf SA, Rajanayagan V, Terpstra M, Merkle H, Truwit CL, Garwood M, Nyberg SL, Uğurbil K. Resolution improvements in in vivo ^{1}H NMR spectra with increased magnetic field strength. J Magn Reson 1998;135:260–264.
10. Gruetter R, Garwood M, Uğurbil K, Seaquist ER. Observation of resolved glucose signals in ^{1}H NMR spectra of the human brain at 4 Tesla. Magn Reson Med 1996;36:1–6.
11. Bartha R, Drost DJ, Menon RS, Williamson PC. Comparison of the quantification precision of human short echo time ^{1}H spectroscopy at 1.5 and 4.0 Tesla. Magn Reson Med 2000;44:185–192.
12. Posse S, Cuenod CA, Risinger R, Le Bihan D, Balaban RS. Anomalous transverse relaxation in ^{1}H spectroscopy in human brain at 4 T. Magn Reson Med 1995;33:246–252.
13. Hetherington HP, Mason GF, Pan JW, Ponder SL, Vaughan JT, Tweig DB, Pohost GM. Evaluation of cerebral gray and white matter metabolite differences by spectroscopic imaging at 4.1 T. Magn Reson Med 1994;32:565–571.
14. Hetherington HP, Pan JW, Mason GF, Adams D, Vaughn MJ, Twieg DB, Pohost GM. Quantitative ^{1}H spectroscopic imaging of human brain at 4.1 T using image segmentation. Magn Reson Med 1996;36:21–29.
15. Pan JW, Twieg DB, Hetherington HP. Quantitative spectroscopic imaging of the human brain. Magn Reson Med 1998;40:363–369.
16. Pan JW, Mason GF, Pohost GM, Hetherington HP. Spectroscopic imaging of human brain glutamate by water-suppressed J-refocused coherence transfer at 4.1 T. Magn Reson Med 1996;36:7–12.
17. Mescher M, Merkle H, Kirsch J, Garwood M, Gruetter R. Simultaneous in vivo spectral editing and water suppression. NMR Biomed 1998;11:266–272.
18. Middleton DA, Hockings PD, Glen S, Reid DG, Rose SE, Crozier S, Roffman W, Rothaul AL, Hunter AJ, Doddrell DM. Image directed proton spectroscopy of gerbil brain at 7 Tesla. NMR Biomed 1995;8:118–126.
19. Penrice J, Lorek A, Cady EB, Amess PN, Wylezinska M, Cooper CE, D'Souza P, Brown GC, Kirkbride V, Edwards AD, Wyatt JS, Reynolds EO. Proton magnetic resonance spectroscopy of the brain during acute hypoxia-ischemia and delayed cerebral energy failure in the newborn piglet. Pediatr Res 1997;41:795–802.
20. Fernandez EJ, Maudsley AA, Higuchi T, Weiner MW. ^{1}H spectroscopic imaging of rat brain at 7 Tesla. Magn Reson Med 1992;25:107–119.
21. Fernandez EJ, Maudsley AA, Higuchi T, Weiner MW. Three-dimensional ^{1}H spectroscopic imaging of cerebral metabolites in the rat using surface coils. Magn Reson Imag 1992;10:965–974.
22. von Kienlin M, Ziegler A, Le Fur Y, Rubin C, Decorps M, Remy C. 2D-spatial/2D-spectral spectroscopic imaging of intracerebral gliomas in rat brain. Magn Reson Med 2000;43:211–219.
23. Pfeuffer J, Tkáč I, Provencher SW, Gruetter R. Toward an in vivo neurochemical profile: Quantification of 18 metabolites in short-echo-time ^{1}H NMR spectra of the rat brain. J Magn Reson 1999;141:104–120.
24. Tkáč I, Starčuk Z, Choi I-Y, Gruetter R. In vivo ^{1}H NMR spectroscopy of rat brain at 1 ms echo time. Magn Reson Med 1999;41:649–656.
25. Provencher SW. Estimation of metabolite concentrations from localized in vivo proton NMR spectra. Magn Reson Med 1993;30:672–679.
26. Adriany G, Yacoub E, Tkáč I, Andersen P, Merkle H, Vaughan JT, Uğurbil K. Shielded surface coils and halfvolume cavity resonators for imaging and spectroscopy applications at 7 Tesla. In: Proc 8th Annual Meeting ISMRM, Denver, 2000. p 563.
27. Merkle H, Driesel W, Andersen P, Adriany G, Uğurbil K, Garwood M. Circularly polarized RF helmet coil for brain studies at 7 Tesla. In: Proc 8th Annual Meeting ISMRM, Denver, 2000. p 565.
28. Gruetter R, Tkáč I. Field mapping without reference scan using asymmetric echo-planar techniques. Magn Reson Med 2000;43:319–323.
29. Seaquist ER, Gruetter R. Identification of a high concentration of scyllo-inositol in the brain of a healthy human subject using ^{1}H and ^{13}C NMR. Magn Reson Med 1998;39:313–316.
30. Govindaraju V, Young K, Maudsley AA, Proton NMR chemical shifts and coupling constants for brain metabolites. NMR Biomed 2000;23:129–153.
31. Terpstra M, Andersen P, Gruetter R. Localized eddy current compensation using quantitative field mapping. J Magn Reson 1998;131:139–143.
32. van der Toorn A, Dijkhuizen RM, Tulleken CA, Nicolay K. T_1 and T_2 relaxation times of the major ^{1}H-containing metabolites in rat brain after focal ischemia. NMR Biomed 1995;8:245–52.
33. Lenz C, Frietsch T, Futterer C, Rebel A, van Ackern K, Kuschinsky W, Waschke KF, Local coupling of cerebral blood flow to cerebral glucose metabolism during inhalational anesthesia in rats: desflurane versus isoflurane. Anesthesiology 1999;91:1720–1723.
34. Gruetter R, Uğurbil K, Seaquist ER. Steady-state cerebral glucose concentrations and transport in the human brain. J Neurochem 1998;70:397–408.
35. Gruetter R, Seaquist E, Kim S-W, Uğurbil K. Localized in vivo ^{13}C NMR of glutamate metabolism. Initial results at 4 Tesla. Dev Neurosci 1998;20:380–388.
36. Shen J, Petersen KF, Behar KL, Brown P, Nixon TW, Mason GF, Petroff OA, Shulman GI, Shulman RG, Rothman DL. Determination of the rate of the glutamate/glutamine cycle in the human brain by in vivo ^{13}C NMR. Proc Natl Acad Sci USA 1999;96:8235–8240.
37. Jenkins BG, Klivenyi P, Kustermann E, Andreassen OA, Ferrante RJ, Rosen BR, Beal MF. Nonlinear decrease over time in N-acetyl aspartate level in the absence of neuronal loss and increases in glutamine and glucose in transgenic Huntington's disease mice. J Neurochem 2000;74:2108–2119.
38. Ellison DW, Beal MF, Martin JB. Amino acid neurotransmitters in postmortem human brain analyzed by high performance liquid chromatography with electrochemical detection. J Neurosci Meth 1987;19:305–315.